Biochimica et Biophysica Acta, 1104 (1992) 137–146

BBAMEM 75518

A ^{31}P-NMR spin-lattice relaxation and ^{31}P{^{1}H} nuclear Overhauser effect study of sonicated small unilamellar phosphatidylcholine vesicles

Joseph S. Tauskela and Michael Thompson

Department of Chemistry, University of Toronto, Toronto, Ontario (Canada)

(Received 28 May 1991)
(Revised manuscript received 16 September 1991)

Key words: Phosphatidylcholine; NMR, ^{31}P-; Nuclear Overhauser effect

The motional properties of the inner and outer monolayer headgroups of egg phosphatidylcholine (PC) small unilamellar vesicles (SUV) were investigated by ^{31}P-NMR temperature-dependent spin-lattice relaxation time constant (T_1) and ^{31}P{^{1}H} nuclear Overhauser effect (NOE) analyses. Three different aspects of the dynamics of PC headgroups were investigated using the T_1 analysis. First, differences in the dynamics of the headgroup region of both surfaces of the SUV were measured after application of a chemical shift reagent, $PrCl_3$, to either the extra- or intravesicular volumes. Second, the ability of the T_1 experiment to resolve the different motional states was evaluated in the absence of shift reagent. Third, comparison between correlation times obtained from a resonance frequency dependent ^{31}P{^{1}H} NOE analysis allowed a determination of the applicability of a simplified motional model to describe phosphorus dipolar relaxation. Temperature-dependent ^{31}P-NMR T_1 values obtained for the individual monolayers at 81.0 and 162.0 MHz were modelled assuming that phosphorus undergoes both a dipolar and an anisotropic chemical shielding relaxation mechanism, each being described by the same correlation time, τ. At 162.0 MHz, the position of the T_1 minimum for the inner monolayer was 9° higher than that of the outer region, indicating a higher level of motional restriction for the inner leaflet, in agreement with ^{31}P{^{1}H} NOE measurements. The 162.0 MHz T_1 profile of the combined SUV monolayers exhibited a smooth minimum located at the midpoint of the monolayer minima positions, effectively masking the presence of the individual surfaces. ^{31}P{^{1}H} NOE results obtained at 32.3, 81.0 and 162.0 MHz did not agree with those predicted from a simple dipolar relaxation model. These results suggest a T_1-temperature method can neither discriminate two or more closely related motional time scales in a heterogeneous environment (such as incorporation of protein into lipid bilayers) nor allow accurate determination of the correlation time at the position of the minimum when the dipolar relaxation rate makes a significant contribution to the overall rate.

Introduction

^{31}P-NMR spin-lattice relaxation time (T_1) determinations have provided considerable insight into the dynamic behaviour of the phosphorus moiety of phospholipid headgroups. Single-temperature T_1 measurements have proved useful in qualitative determinations of the effects which various reconstituted or membrane-soluble proteins have on lipid headgroups [1–5], and also in comparisons between the individual monolayers which constitute small unilamellar vesicles (SUV) [6]. More detailed temperature-dependent ^{31}P-NMR T_1 examinations [7–13] have elicited much interest since a minimum relaxation time constant was observed in all cases. This finding allows estimation of the rates of the dominant motions that are present at the temperature where the minimum occurs because this is the region where the spectral density function for the phosphorus is the greatest. Furthermore, semi-quantitative information on the motional rates could be obtained since at the position of the minimum, for

Correspondence (at present address): J.S. Tauskela, Montreal Neurological Institute, McGill University, 3801 University Ave., Montreal, Quebec, Canada, H3A 2B4.

the relaxation mechanisms involved the correlation time, τ, is on the order of the inverse of the Larmor resonance frequency, ω; i.e., $\omega\tau \approx 1$.

This relationship is, however, only approximate since more exact determination of the relationship of τ_{min} to ω requires a knowledge of the individual relaxation mechanisms, and the types of motions responsible for generating the relaxation. At the elevated magnetic field strengths that are required to obtain a phospholipid T_1 minimum at a temperature greater than 0°C, two processes are responsible for the observed relaxation rate, the dipole-dipole ($T_{1,DD}^{-1}$), and chemical shielding anisotropy ($T_{1,CSA}^{-1}$) rates [10]. Since the latter process is proportional to the magnetic resonance frequency employed, elucidation of the individual rates can be obtained from data gathered at a number of different frequencies. Fitting of these data to an appropriate relaxation model yields a value for τ_{min}.

Since only a single minimum has been found for phospholipid dispersions, a model has been employed in which it is assumed that the phosphorus headgroup undergoes a single unrestricted isotropic motion [7–14]. The τ_{min} values obtained by this procedure probably represent an average of interactions, since it is known that the relaxation of phosphorus is much more complex than depicted in this model. For instance, Milburn and Jeffrey [14] have shown that there is a dependence of the ^{31}P-NMR T_1 time constants at elevated resonance frequencies on the angle between the magnetic field and the bilayer in oriented multilayers, reflecting the anisotropic nature of the phosphorus motion. At least three different contributions are believed to be important in the dipolar relaxation of the ^{31}P nucleus, including an intramolecular interaction from the choline methylene protons, an intermolecular interaction with the choline N-methyl protons [15–18] and contributions from the H_2O protons [11].

One of the major advantages often cited for employing a T_1-temperature analysis is that information can be obtained regarding the effect of perturbant molecules (such as proteins, different lipids, and steroids) by monitoring the change in the position of the minimum [7–9,13]. However, conclusions regarding any movement in the position of the minimum must be treated cautiously since in heterogeneous dispersions there may be more than one distinct lipid environment. For instance, it has been suggested that the lipid that is in contact with a protein may experience some immobilization [5]. No studies have yet reported differences in τ_{min} for the same phospholipid existing in two well-characterized environments.

In this study, a comprehensive analysis of phosphatidylcholine (PC) headgroup ^{31}P-NMR spin-lattice relaxation behaviour has been performed. To avoid the uncertainties associated with an examination of ill-defined lipid environments in proteinaceous multilamellar systems, SUV have been employed. In these structures, the intense surface curvature causes the inner and outer halves (the individual monolayers making up the bilayer) to become highly asymmetric with respect to molecular packing [19–22], resulting in differences in the conformations and dynamic behaviour. ^{31}P-NMR temperature-dependent T_1 measurements were performed at two different resonant frequencies for each monolayer making up the SUV in order to isolate the relative contributions of the DD and CSA relaxation mechanisms, thereby enabling τ_{min} to be determined. Relative contributions of DD and CSA rates to overall relaxation rates determined from T_1 measurements did not correlate with ^{31}P{^{1}H} NOE results, indicating that a simple motional model for DD relaxation yields inaccurate estimations for τ values. Finally, a T_1-temperature analysis of the combined monolayers revealed only a single minimum where two were known to exist (one for each monolayer), implying that lipids existing in different environments can easily be mistaken for a homogenous type.

Materials and Methods

Lyophilized egg L-α-phosphatidylcholine was obtained from Avanti Polar Lipids and $PrCl_3$ from Alfa Division. To prepare the SUV the lipid (up to 1 g) was dissolved in methanol and the solvent evaporated using a rotary evaporator, leaving a thin lipid film which was then exposed to a nitrogen stream until dry. This film was dissolved in 10 mM Hepes buffer (100 mg lipid/ml) and the solution adjusted to pH 7.3. To those solutions to which $PrCl_3$ was added the pH was slightly acidic by 0.2 units. To avoid auto-oxidation and chemical degradation solutions were kept under nitrogen and stored in the dark at 5°C for up to 24 h before use.

A Vibra Cell Sonicator (Sonics Materials Inc.) equipped with a titanium probe tip was used to prepare the SUV. Sample volumes (5 ± 2 ml) required 60 min at a power setting of 3.5 to obtain a clear blue opalescent solution. Nitrogen was bubbled into the sample during the procedure and a cold water jacket was used to prevent heating. After preparation, the sample was centrifuged for 30 min at 20000 rpm at 15°C to remove any multilamellar components. Vesicle samples were sealed under a nitrogen atmosphere and kept in the dark for no more than 24 h before use. Gel filtration employing a 2.5×50 cm column packed with Sephacryl S-1000 gel (Pharmacia, Montreal) yielded a profile in which the major component was skewed towards smaller sizes. Quasielastic laser light scattering of the fraction located at the peak of the profile yielded SUV diameters of 58 ± 1 nm.

To isolate the inner monolayer resonance, 1 mM $PrCl_3$ was added to the solution. To isolate the outer monolayer resonance 1 mM $PrCl_3$ was added to the multilamellar dispersion before sonication. After this

procedure, the extra-vesicular chemical shift reagent was removed through passage of a 2.5 × 50 cm column packed with Sephadex G-25–50 gel (Pharmacia, Montreal), pretreated with lipid [19].

^{31}P-nuclear magnetic resonance experiments were performed at three resonant frequencies: 32.3 MHz (Bruker WP-80), 81.0 MHz (Varian XL-200) and 162.0 MHz (Bruker WH-400), all in 10 mm sample tube sizes. ^{31}P-NMR spin-lattice relaxation time constant (T_1) measurements were carried out by the inversion recovery method and a minimum of thirteen different delay values was employed for all measurements. At 81.0 MHz, T_1 values were obtained from a non-linear least-squares fit to

$$S_t = S_\infty(1 - 2e^{-t/T_1}) \quad (1)$$

where S_∞ is the thermal magnetization value and S_t is the magnetization value for that particular t value employed. At 32.3 and 162.0 MHz T_1 values were calculated from the slope of a plot of $\ln(S_\infty - S_t)$ vs. t. At 25°C typically the number of scans for each delay was set to 100 at 32.3 MHz, 40 at 81.0 MHz and to 48 at 162.0 MHz. At lower temperatures it was necessary to increase this number while at higher temperatures the value was usually less. Pulse width (2π) determinations were made for every temperature or sample change that was performed. Since long T_1 experiments are particularly sensitive to long-term changes in magnet homogeneity, short and long t values were alternated or interleaved.

Two methods were used to measure the ^{31}P{^{1}H} NOE's. In one, the broadband ^{1}H decoupler was on all the time and the signal was compared to the ^{31}P spectrum obtained with the decoupler gated on only during acquisition of the ^{31}P signal [23,24]. Alternatively, the proton decoupler was turned off immediately before the ^{31}P excitation pulse and was restored just after the ^{31}P receiver had finished acquiring the free induction decay signal [25,26]. This signal was compared with the ^{31}P spectrum obtained without proton decoupling. Pulse intervals of at least 5 T_1 following data acquisition were used for both procedures. Peak areas were evaluated using a planimeter or by cutting and weighing copies of the spectra. The magnitudes of the NOE's are reported as percentages with 124% the maximum possible enhancement.

Results

T_1-temperature experiments

The inner and outer monolayer ^{31}P-NMR resonances of the PC SUV were not well resolved at any temperature to determine T_1 time constants at the chosen resonant frequencies (81.0 and 162.0 MHz). This necessitated the use of the chemical shift reagent, 1 mM $PrCl_3$, which caused a downfield shift (≈ 15 ppm) of the monolayer to which it was exposed, thereby allowing measurements to be made on the other unaffected leaflet. Since this paramagnetic reagent causes a significant reduction in the spin-lattice relaxation times it was necessary to ensure that no leakage of Pr^{3+} occurred across the bilayer to the monolayer of interest. Although numerous bilayer vesicle studies which have employed this reagent report no leakage [6,27,28], all were performed at room temperature, not at the range that was required in this study. To complex any free Pr^{3+} ions, 1 mM EDTA was added to the appropriate side of the vesicle [15]. Several lines of evidence suggest that unwanted contact between the headgroups and the Pr^{3+} ions did not occur:

(i) the chemical shift difference between shifted and unshifted ^{31}P monolayer resonances, which varies as a function of concentration [28], did not vary as a function of temperature,

(ii) integration of the two resonance peaks did not vary with temperature,

(iii) linewidths continually narrowed as higher temperatures were employed, which would not result if Pr^{3+} leakage had occurred,

(iv) T_1 measurements determined after a series of high or low temperatures were no different than pre-experiment controls at room temperature.

The ^{31}P-NMR T_1 relaxation profiles for the inner and outer monolayers of the SUV samples measured at 81.0 and 162.0 MHz are shown in Fig. 1 (along with the curves generated by a fitting analysis, discussed in the next section). T_1 time constants were significantly higher at the lower magnetic resonance frequency for any one temperature on the high temperature region of the curves. This trend is consistent with the chemical shielding anisotropy mechanism making a contribution to the overall relaxation process, at least for the T_1 time constants determined at 162.0 MHz [10]. Dipolar relaxation predicts similar T_1 values for both frequencies on the high temperature side of the minimum. Thus, determinations of the correlation times for the phosphorus motion from the 162.0 MHz T_1 data have to take into account that both dipolar and chemical shielding anisotropy relaxation mechanisms exist. The T_1 time constants measured at 32.3 MHz at 25°C (not shown) were also higher than those measured at the higher frequencies, indicating that at 81.0 MHz a chemical shielding anisotropy term must also be invoked to adequately describe the relaxation of the phosphorus.

Fitting of the isotropic motional model to the T_1-temperature data of the individual SUV monolayers

At the resonant frequencies employed, the spin-lattice relaxation rate is given by

$$1/T_{1,\text{overall}} = 1/T_{1,\text{DD}} + 1/T_{1,\text{CSA}} \quad (2)$$

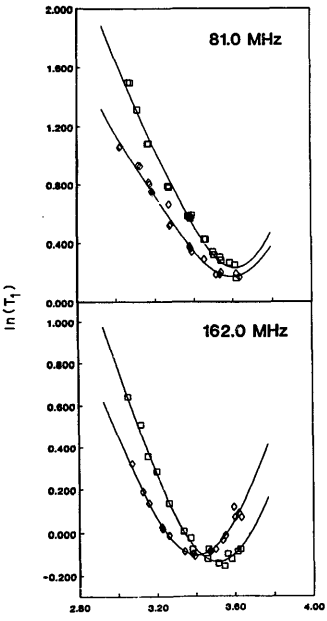

Fig. 1. ^{31}P-NMR spin-lattice relaxation times measured at 81.0 and 162.0 MHz for the chemically shifted inner (○) and outer (□) monolayers of egg PC SUV as a function of temperature. The data has been fit to the sum of DD and CSA relaxation rates, assuming an isotropic motional model for each mechanism. The relaxation times for each monolayer are quite distinct at both resonant frequencies and the data is fit quite well using a single correlation time model.

To calculate these two terms, it has been simplistically assumed that the phosphorus moiety is undergoing isotropic rotational diffusion and can be modelled by a single correlation time, τ. For this situation the spectral density function, $J(\omega)$, is [29]

$$J(\omega) = \tau(1+\omega_P^2\tau^2)^{-1} \tag{3}$$

where ω_P is the resonant frequency for the ^{31}P resonance. Assuming this type of interaction, this yields the function [30]

$$1/T_{1,DD} = (1/10)K^2r^{-6}[J_0(\omega_H-\omega_P)+3J_1(\omega_P)+6J_2(\omega_H+\omega_P)] \tag{4}$$

and [29]

$$1/T_{1,CSA} = (3/10)\omega_P^2\Delta\sigma^2\left(\frac{\tau}{1+\omega_P^2\tau^2}\right) \tag{5}$$

where r represents the ^{31}P-^{1}H internuclear distance, ω_H is the resonant frequency for the ^{1}H resonance, $K = \hbar\gamma_{^{31}P}\gamma_{^1H}$ and $\Delta\sigma$ is the residual chemical shielding anisotropy. As in the study of Milburn and Jeffrey [10], these latter two values were parameters determined from the data. Finally, to determine the values of the correlation times over the temperature range examined, it was assumed that the motions of the phosphorus have an Arrhenius dependence with temperature, as given by

$$\ln\tau_i = \ln\tau_0 - E_a/RT \tag{6}$$

where τ_0 is the correlation time at infinite temperature, E_a is the activation energy, R is Boltzmann's constant and T is the temperature in degrees Kelvin.

Four independent parameters were used in fitting the T_1 versus temperature curves (Table I): (i) the term, $K^2/10r^6$, from Eqn. 4; (ii) the term, $0.3\Delta\sigma^2$, from Eqn. 5 (which has been divided by ω_P^2 to eliminate the magnetic field strength dependence); (iii) τ_0 and (iv) E_a, both from Eqn. 6. The fitting procedure was based on the downhill simplex method of Nelder and Mead [31] for multidimensional minimization [32].

TABLE I

Fitting parameters from ^{31}P-NMR T_1-temperature data of the individual monolayers of egg PC SUV

Resonant frequency (MHz)	Monolayer	$K^2/10r^6$ ($\times 10^8$)	$0.3\Delta\sigma^2/\omega_P^2$ ($\times 10^{-9}$)	τ_0 (fs)	E_a/R
162.0	inner	1.35 ± 0.05	1.74 ± 0.01	3.13 ± 0.22	3036 ± 20
	outer	4.33 ± 1.51	2.10 ± 0.10	1.69 ± 0.27	3123 ± 45
81.0	inner	1.10 ± 0.03	1.88 ± 0.04	1.10 ± 0.12	3356 ± 30
	outer	6.50 ± 0.21	2.25 ± 0.00	1.36 ± 0.06	3922 ± 11

TABLE II

^{31}P-NMR activation energies for the inner and outer monolayers of egg PC SUV and DPPC micelles

Preparation	Activation energy (kcal/mol)	
	81.0 MHz	162.0 MHz
SUV inner monolayer	6.67 ± 0.06	6.04 ± 0.04
SUV outer monolayer	7.80 ± 0.02	6.21 ± 0.09
DPPC micelles	3.54 ± 0.05	3.05 ± 0.05

Due to the uncertainty in the position of the T_1 minima for the 81.0 MHz data, the data obtained at each resonance frequency were fit to the rate equations independently.

Of particular importance are the differences in the $K^2/10r^6$ terms for the two monolayers because of the r dependence, and the Arrhenius activation energies. Table II separately lists the calculated activation energies along with those that were obtained for a PC system, dipalmitoylphosphatidylcholine (DPPC) micelles, in methanol. In organic solvents, PC molecules are believed to have a less hindered rotation than for the bilayer form [33], so this system allowed a comparison to be made with the energies obtained for the monolayers from the fitting analysis.

Each of the inner and outer monolayer T_1 versus temperature plots that were obtained at 81.0 and 162.0 MHz were fit using these parameters. Fig. 1 indicates that an excellent fit to the data was generated at both resonant frequencies. At both field strengths it is clear that a distinctive well-defined minimum is present for each monolayer and, in addition, at 162.0 MHz there is a significant difference in the position of the two monolayers.

Fitting of the isotropic motional model to the T_1-temperature data for the combined SUV monolayers

The T_1-temperature curve for the combined monolayers was determined in the absence of shift reagent (Fig. 2). At 162.0 MHz, the spectral shape was a single signal at all temperatures due to CSA broadening contributions of the linewidth [34,35]. Although it was shown that two minima exist (Fig. 1), the data obtained for the combined monolayers did not display this type of profile. Since the location of each minimum position could not be adequately resolved from the data, modelling was performed only in terms of a single correlation time. It is clear that a very good fit to the data was obtained by assuming that only a single minimum exists, essentially hiding the dual nature of the relaxation profile.

Fig. 3 compares the 162.0 MHz egg PC individual monolayer curves with the combined curve. From this comparison, it is evident how such an effective masking of the two components could occur. The position of the minimum for the dual monolayers is located midway between that of the inner and outer minima positions. The combined system has a broader profile which essentially encompasses the total width of both profiles.

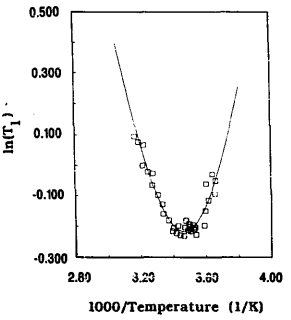

Fig. 2. Isotropic dynamic model fitting to ^{31}P-NMR T_1-temperature data obtained at 162.0 MHz for combined monolayers of egg PC SUV. The data fit quite well assuming only a single correlation time exists.

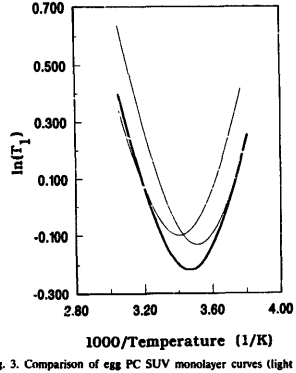

Fig. 3. Comparison of egg PC SUV monolayer curves (light lines) with combined monolayer curve (bold line) obtained from fittings of the 162.0 MHz T_1-temperature data. The combined curve displays a minimum at a position midway between that of the individual curves and is significantly broader, essentially as wide as the combination of the two curves.

$^{31}P\{^1H\}$ Nuclear Overhauser effect enhancements of SUV monolayers

$^{31}P\{^1H\}$ NOE experiments were initially performed at a relatively low magnetic resonant frequency, 32.3 MHz, for both monolayers. It has been shown by Ycagle et al. [15] that at this level relaxation of the phosphorus nucleus occurs predominantly by a dipolar mechanism. This is in principle a simpler method of comparing the phosphorus correlation time between monolayers since only one relaxation mechanism need be considered and there is no direct dependence of the NOE on the distance between dipolar coupled nuclei, as there is for the dipolar T_1 relaxation process. For the isotropic model, τ can be calculated from observed NOE enhancements (NOEE)

NOEE

$$= 1 + \frac{\gamma_H}{\gamma_P}\frac{\left[\dfrac{6\tau}{1+(\omega_H+\omega_P)^2\tau^2} - \dfrac{\tau}{1+(\omega_H-\omega_P)^2\tau^2}\right]}{\left[\dfrac{\tau}{1+(\omega_H-\omega_P)^2\tau^2} + \dfrac{3\tau}{1+\omega_P^2\tau^2} + \dfrac{6\tau}{1+(\omega_H+\omega_P)^2\tau^2}\right]} \quad (7)$$

NOEE obtained for each surface at 25°C and calculated τ values are given in Table III. The NOEE calculated from Eqn. 7 is significantly higher for the outer monolayer, while the correlation time is shorter (1.24 ns) for this region compared to the inner surface value (1.63 ns).

$^{31}P\{^1H\}$ NOEE were also measured at 81.0 and 162.0 MHz (Table IV). The decreases seen with respect to the 32.3 MHz data are the result of two mechanisms, motional attenuation of the dipolar mechanism due to the extreme narrowing condition not holding under these conditions for SUVs, and a decline in the dipolar relaxation contribution to the overall rate (resulting from the increasing importance of the CSA rate at these elevated frequencies). The relative contribution of each of these terms to the observed decrease can be determined from the following equation

$$NOEE_{observed} = (NOEE_{theoretical})(T_{1,DD}^{-1} / T_{1,overall}^{-1}) \quad (8)$$

TABLE III

Calculated correlation times from 32.3 MHz $^{31}P\{^1H\}$ NOE enhancements of egg PC SUV inner and outer monolayers at 25°C

Parameter measured	Inner monolayer	Outer monolayer
NOE enhancement (±10%)	42	56
τ_c (ns)	1.63	1.24

TABLE IV

Observed versus predicted $^{31}P\{^1H\}$ NOE enhancements for inner and outer monolayers of egg PC SUV at 25°C

Resonant frequency (MHz)	Observed NOEE (±10%)		Predicted [a] NOEE (±10%)	
	inner	outer	inner	outer
81.0	21	31	14	19
162.0	12	12	8	10

[a] Determined from Eqn. 7 by employing the τ values obtained from the 32.3 MHz NOEE given in Table III. Errors were assumed to be the same as for the observed enhancements.

Measurement of this decline in the NOEE at higher resonance frequencies thus provides an alternative to the T_1 data fitting procedure for determining the relative contributions of DD and CSA relaxation mechanisms to overall T_1 relaxation.

The first step in elucidating the two contributions was to determine the NOE decrease solely in terms of the dipolar mechanism. Correlation times obtained at 32.3 MHz (Table III) were used to predict NOEE at 81.0 and 162.0 MHz (Table IV). The predicted motionally attenuated values were either within the experimental error of the measurements or less than those observed, indicating no contribution from CSA. Since much higher NOEE were expected, this suggests that the correlation times obtained from the 32.3 MHz data should have been significantly shorter than were calculated.

The source of the $^{31}P\{^1H\}$ NOE in PC SUV monolayers

Previous $^{31}P\{^1H\}$ NOE studies on phospholipid vesicles have suggested that intra- and intermolecular ^{31}P-^1H dipolar relaxation processes occur [15–18]. However, these studies only examined the combined monolayers in SUV and not the individual monolayers. To confirm that there is more than one interaction contributing to a dipolar relaxation mechanism for both monolayers, the $^{31}P\{^1H\}$ NOEE of SUV in which the *N*-methyl choline protons of palmitoyl-oleoyl-PC (POPC) were substituted by deuterium (i.e., the terminus was $(CD_3)_3$-N^+-POPC to give γ_{d9}-POPC) were examined. Since substitution of a proton by a deuterium removes the ^{31}P-^1H dipolar cross-relaxation that is in part necessary to generate an NOE, it was expected that a decrease in NOEE would be observed if the *N*-methyl choline protons were contributing. Once again, the chemical shift reagent, $PrCl_3$, was employed to isolate the monolayer of interest. Results from this analysis (Table V) show that there was a significant decrease in the enhancements upon deuteration for both the inner monolayer (from 21% to 12%) and outer region (from 31% to 23%). This indicates that the *N*-methyl choline protons do contribute to the

TABLE V

Comparison between 81.0 MHz $^{31}P\{^1H\}$ NOE enhancements for γ_{do}-POPC and egg PC SUV monolayers at 25°C

Preparation	NOE enhancement (±10%)	
	inner monolayer	outer monolayer
Egg PC SUV	21	31
γ_{do}-POPC SUV	12	23

$^{31}P\{^1H\}$ NOE. Since an NOE still remains for both surfaces, there is an additional contribution to the dipolar relaxation process.

Discussion

^{31}P-NMR T_1 measurements of PC SUV individual monolayers: relaxation rate equation fitting to data

In this study, the two monolayers which make up SUV were investigated independently by a temperature-dependent ^{31}P-NMR spin-lattice relaxation time analysis. The fact that a clear difference exists in the position of the T_1 minimum with respect to temperature (at 162.0 MHz) allowed two different types of analyses to be performed. First, differences in the motional properties between monolayer headgroups were examined in a quantitative manner by fitting each of the monolayer T_1 data to DD and CSA relaxation rate equations. To describe these relaxation processes, it was assumed that the phosphorus moiety undergoes isotropic reorientation. $^{31}P\{^1H\}$ NOE experiments were performed as an independent measure of the relative contribution of the dipolar and chemical shielding anisotropic relaxation mechanisms to the overall T_1 relaxation. Comparison of the τ values calculated from these two techniques allowed a measure of the applicability of a simplified motional model to describe phosphorus DD relaxation. Second, the ability of the T_1 experiment to resolve the different motional states was evaluated in the absence of shift reagent.

The dependence of the T_1 time constants on frequency at high temperature indicates that both DD and CSA relaxation rate equations are needed to obtain an estimation of τ_{min}. Table VI summarizes the relevant minima parameters obtained from the T_1 experiments and the fitting of Eqn. 2 to this data. For each resonant frequency, the τ_{min} is the same for both surfaces. This was expected since at the minimum, $\omega\tau_{min} \approx 1$, so τ_{min} is only a function of the resonant frequency employed. The temperature corresponding to the minimum spin-lattice relaxation time is significantly higher (9.0°C) for the inner monolayer compared to the outer leaflet. This implies that the inner surface phosphorus has an increased spectral density of lower frequency motions compared to the outer monolayer. The time-scale of the molecular motion of the PC molecule is too slow to cause effective spin-lattice relaxation at the magnetic field strengths employed [36] so this observation likely reflects differences in the segmental motions of the headgroup [10]. This confirms the proposal made in previous theoretical [19–22] and experimental [6] studies that the inner region phosphorus undergoes slower and therefore more restricted motions on average compared to the outer surface.

TABLE VI

SUV ^{31}P-NMR T_1-temperature minima parameters

Frequency (MHz)	Monolayer	τ_{min} (ns)	$T_{1,min}$ (s)	$Temp_{min}$ (°C)
162.0	inner	1.0	0.90	20.5
	outer	1.0	0.88	11.5
81.0	inner	1.9	1.19	5.5
	outer	1.9	1.27	4.0

The displacement of the T_1 minima towards lower temperatures at the lower resonant frequency employed (81.0 MHz) is due not only to the dependence of the dipolar relaxation rate on ω_P (Eqn. 4) but also to chemical shielding anisotropy. As a result of the field dependence of CSA, the relative contribution of the $T_{1,CSA}^{-1}$ term to the overall rate in Eqn. 2 differs at 81.0 and 162.0 MHz. The relationship between ω_P and τ at the minimum differs between the DD and CSA relaxation mechanisms. Thus, different relative contributions of each relaxation mechanism alter the position of the minimum.

There are a number of differences between the fitting parameters generated from the 81.0 and 162.0 MHz data. Table VI indicates that the position of the minima for the inner monolayer changes by 15° in going from one resonance frequency to the other but changes only by 7.5° for the outer monolayer. This may be partly due to the change in the efficiency of CSA relaxation between the two field strengths employed, but it is most likely due to the lack of data near the minimum region (at 81.0 MHz), making accurate assignment difficult. The uncertainty in the position of the minimum at 81.0 MHz is also probably responsible for the activation energies determined at this frequency being significantly higher than those determined from the 162.0 MHz data.

E_a values determined from the 162.0 MHz data are quite similar, implying that the movement of the T_1 minimum may be a much more sensitive indicator of the differences in headgroup motional properties. For PC systems in which there are greater differences, though, the activation energies do follow the expected trend. Comparison with E_a values for methanol shows the expected change since these values are lower than that of either monolayer (Table II); in solution the

micelles exist in trimer form [33] and are therefore not subject to the motional restrictions that exist in the monolayer. Ghosh [12] has examined phospholipid ^{31}P-NMR activation energies as a function of spacing between headgroups created by introduction of cholesterol and found that these values followed the expected trend by decreasing as the intermolecular distance increased. The $K^2/10r^6$ term determined from the fitting analysis provides a measure of the distance between the phosphorus and a dipolar coupled proton. The actual r values obtained from this type of procedure are subject to considerable uncertainty since more than one proton is involved and the $^{31}P\{^1H\}$ NOE results (Table IV) reveal that at least two sources of protons contribute to phosphorus dipolar relaxation exist. If it is assumed that the dipolar relaxation of the ^{31}P nucleus is dominated by the interaction with its nearest neighbor, then the r value obtained will represent the weighted average of the distances involved. One interesting comparison that can be made is the ratio of the outer:inner r value, which is significantly greater than unity (21% and 35% higher as determined at 162.0 and 81.0 MHz, respectively). This implies that differences do exist in the average distance between dipolar coupled ^{1}H-^{31}P nuclei in the inner and outer monolayer surface. If this is a reflection of the greater separation that is believed to exist between outer monolayer headgroups, this would imply that processes other than intermolecular dipolar proton–phosphorus interactions do not differ appreciably for the two surfaces.

^{31}P-NMR T_1 measurements of PC SUV combined monolayers

A single minimum at 162.0 MHz was observed for the SUV samples to which no shift reagent was added, located close to the midpoint of the position of the separated monolayers (Fig. 2). The curve for the combined system is essentially a linear combination of the two individual curves, indicating that the overall relaxation rate represents the sum of the relaxation rates of the monolayers. On the high temperature side of the minimum the inner surface relaxation rates dominates, while on the low temperature side the outer monolayer has the most efficient phosphorus relaxation. Thus, the effect of more than one interaction contributing to the relaxation of the ^{31}P nucleus is to broaden the T_1 minimum observed. Although the amplitudes of T_1 values at the minimum of the individual monolayers are quite similar, the amplitude of the combined monolayers is less than the both of them (Fig. 3). Since one would not expect any differences between these two forms, this is most likely due to fitting to two partially overlapping minima; i.e., the combined SUV data has a broader minimum and this may alter the amplitude of the minimum.

Since a distinctive minimum clearly does exist for each monolayer at 162.0 MHz, this implies the presence of two components may not be detectable in a T_1-temperature analysis. This finding has important repercussions for T_1-temperature analyses of lipid-protein dispersions or for any other dispersion in which it may be believed that more than one dynamically different lipid component exists. The presence of a single mimimum may in fact represent a distribution of closely related correlation times so this method can not be used to prove that only a single environment exists.

$^{31}P\{^1H\}$ NOE enhancements of PC SUV individual monolayers

The $^{31}P\{^1H\}$ nuclear Overhauser effect enhancements for the outer surface ($56 \pm 10\%$) is greater than the value obtained for the inner region ($42 \pm 10\%$). From Eqn. 7, this yields a longer correlation time for the inner phosphorus (1.63 ns) compared to the outer one (1.24 ns). Since the NOE depends only on the τ value for the phosphorus this confirms that the motion of the inner phosphorus is hindered to some degree, in agreement with the conclusion reached from the T_1 relaxation data.

These correlation times were used to predict the $^{31}P\{^1H\}$ NOE enhancements that should be seen at the two other resonant frequencies employed in this study, 81.0 and 162.0 MHz, if a dipolar relaxation mechanism were solely operative. Eqn. 7 was used so these predicted values (Table IV) are based solely on a dipolar relaxation mechanism. There is a decrease in the predicted NOE values at 81.0 MHz and again at 162.0 MHz compared to those at 32.0 MHz and this can be compensated for exclusively by the change in ω_P in Eqn. 7. These values are within experimental error of the measurements or are less than those observed. This was an unexpected result because it is known that CSA relaxation is important at these higher frequencies. This would cause an attenuation of the NOE (Eqn. 8) so the NOEE predicted solely from a dipolar relaxation mechanism should have been significantly larger than those observed. In fact, from the fitting procedure of the relaxation data, the NOEE predicted from Eqn. 7 should be 54% and 69% greater at 81.0 MHz and 80% and 93% greater at 162.0 MHz than the observed NOEE for the outer and inner surfaces, respectively. The fact that a CSA relaxation mechanism does not need to be invoked to account for the measured NOEE when one clearly does exist implies that the DD relaxation model is incorrect. Since the same spectral density function (Eqn. 3) is used in both the $^{31}P\{^1H\}$ NOE and $T_{1,DD}$ expressions, this in turn implies that the correlation times derived from the fitting of the relaxation rate equations to the T_1 data are also inaccurate, at least at 81.0 MHz where the DD rate forms a significant contribution to the overall rate.

The most likely cause of this discrepancy is the use of a single correlation time model since there are a number of interactions which play a role in the relaxation of the phosphorus nucleus. The headgroup N-methyl choline protons are involved in a dipolar relaxation mechanism for both surfaces, based upon the observation that there is a decrease in the enhancements from the respective non-deuterated monolayers of 43% and 26% for the inner and outer monolayers, respectively (Table V). A conclusion regarding this difference in relative decreases observed can not be made with any certainty, though, since the absolute intensities of these enhancements is rather small, being in the range of only 10–20% of the theoretical maximum. The remaining NOE enhancement may be due to contributions from the methylene protons [15–17], as well as from the solvent H_2O protons [11]. Thus, the main conclusion that can be drawn from the NOE data is there is more than one contribution to the dipolar relaxation mechanism and that this is responsible for the poor correlation between observed and predicted NOE enhancements at the elevated frequencies.

For the 0° to 60°C temperature range, at 162.0 MHz the fitting analysis yielded a 94% to 90% and 81% to 74% percentage contribution of the CSA relaxation rate to the overall rate for the outer and inner monolayers, respectively. The uncertainty associated with the DD rate equation makes these values only approximate but it can still be concluded that the CSA rate dominates at this resonance frequency. Thus, it is possible that the fitting analysis to the T_1 data yielded more accurate τ values than the $^{31}P\{^1H\}$ NOEE method, even though the same spectral density function was used for both relaxation mechanisms. Similar τ values have been determined in PC multilamellar dispersions by assuming the dominant phosphorus motion is either isotropic reorientation (≈ 3.0 ns at 25°C determined by measurement of temperature and frequency dependences [10]) or axially symmetric rotation (≈ 3.5 ns determined by an orientational dependent analysis [14]). Of course, it must be recognized that this is still a simplified model, given the complexity of the segmental motional rates and amplitudes in the headgroup.

Finally, it is of value to compare T_1 times for SUV with data obtained from multilamellar dispersions. An unambiguous interpretation of the monolayer most closely resembling the planar situation can be obtained by comparison of the positions of the T_1 minima. Milburn and Jeffrey [10] observed a minimum at 10°C at 145.7 MHz for PC multilamellar dispersions, which is much closer to the outer monolayer minimum at 11.5°C determined at 162 MHz (Table VI). (It is expected that the multilamellar minimum position would increase 2–4 C° if measurements were perfomed at 162.0 MHz, which still leaves a better correlation with the outer leaflet minimum position.) This implies that the motional properties of the outer monolayer phosphorus nuclei more closely resemble those existing in planar systems. This indicates that for the sizes of SUV employed (58 nm in diameter), packing constraints for the inner monolayer are more important in altering headgroup dynamic behaviour than the changes caused by the large volume allowed for outer leaflet headgroup movements. This result is not in agreement with calculations by Chrzeszcyk and co-workers [21] which indicated that inner monolayer headgroup conformations more resemble planar configurations, based on area-per-headgroup considerations. This discrepancy may be due to much smaller SUV being employed in that study (22 nm in diameter). In smaller SUV, the volume each outer monolayer headgroup occupies is much larger and this may result in a greater deviation from planar headgroup behaviour than the changes undergone in the inner region.

Acknowledgements

Support for this work from the Natural Sciences and Engineering Research Council is gratefully acknowledged. The University of Guelph NMR Centre is acknowledged for the use of the 400 MHz instrument and Bill Klimstra is thanked for his experimental help. Dr. Peter McDonald of the University of Toronto is gratefully thanked for his gift of the deuterated lipid.

References

1 Rajan, S., Kang, S.Y., Gutowsky, H.S. and Oldfield, E. (1981) J. Biol. Chem. 256, 1160–1166.
2 Deese, A.J., Dratz, E.A. and Brown, M.F. (1981) FEBS Lett. 124, 93–99.
3 Smith, R., Cornell, B.A., Keniry, M.A. and Separovic, F. (1983) Biochim. Biophys. Acta 732, 492–498.
4 Selinsky, B.S. and Yeagle, P.L. (1985) Biochim. Biophys. Acta 813, 33–50.
5 Yeagle, P.L. and Kelsey, D. (1989) Biochemistry 28, 2210–2215.
6 Berden, J.A., Barker, R.W. and Radda, G.K. (1975) Biochim. Biophys. Acta. 375, 186–208.
7 Seelig, J., Tamm, L., Hymeland, L. and Fleischer, S. (1981) Biochemistry 20, 3922–3932.
8 Banaszak, L.J. and Seelig, J. (1982) Biochemistry 21, 2436–2443.
9 Tamm, L.K. and Seelig, J. (1983) Biochemistry 22, 1474–1483.
10 Milburn, M.P. and Jeffrey, K.R. (1987) Biophys. J. 52, 791–799.
11 Milburn, M.P. and Jeffrey, K.R. (1990) Biophys. J. 58, 187–194.
12 Ghosh, R. (1988) Biochemistry 27, 7750–7758.
13 Fenske, D.B., Chana, R.S., Parmar, Y.I., Treleaven, D. and Cushley, R.J. (1990) Biochemistry 29, 3973–3981.
14 Milburn, M.P. and Jeffrey, K.R. (1989) Biophys. J. 56, 543–549.
15 Yeagle, P.L., Hutton, W.C., Huang, C.H. and Martin, R.B. (1975) Proc. Natl. Acad. Sci. USA 72, 3477–3481.
16 Yeagle, P.L., Hutton, W.C., Huang, C.H. and Martin, R.B. (1976) Biochemistry 15, 2121–2124.
17 Yeagle, P.L., Hutton, W.C., Huang, C.H. and Martin, R.B. (1977) Biochemistry 16, 4344–4349.

18 Burns, R.A., Stark, R.E., Vidusek, D.A. and Roberts, M.F. (1983) Biochemistry 22, 5084–5090.
19 Huang, C. (1969) Biochemistry 8, 344–352.
20 Huang, C., Sipe, J.P., Chow, S.T. and Martin, R.B. (1974) Proc. Natl. Acad. Sci. USA 71, 359–362.
21 Chreszczyk, A., Wishnia, A. and Springer, C.S. (1977) Biochim. Biophys. Acta 470, 161–169.
22 Huang, C. and Mason, J.T. (1978) Proc. Natl. Acad. Sci. USA 75, 308–310.
23 Freeman, R. and Hill, H. (1970) J. Magn. Res. 5, 278–280.
24 Freeman, R., Hill, H. and Kaptein, R. (1972) J. Magn. Res. 7, 327–329.
25 Gansow, O.A. and Schiftenhelm, W. (1971) J. Am. Chem. Soc. 93, 4294–4295.
26 Freeman, R. (1970) J. Chem Phys. 53, 457–458.
27 Bystrov, V.F., Dubrovina, N.I., Barsukov, L.J. and Bergelson, L.D. (1971) Chem. Phys. Lipids 6, 343–350.
28 Hutton, W.C., Yeagle, P.L. and Martin, R.B. (1977) Chem. Phys. Lipids 19, 255–265.
29 Abragam, A. (1961) The Principles of Nuclear Magnetism, pp. 424–427, The Oxford University Press, London.
30 Doddrell, D., Glushko, V. and Allerhand, A. (1972) J. Chem. Phys. 56, 3683–3689.
31 Nelder, J.A. and Mead, R. (1965) Computer J. 7, 308–313.
32 Press, W.H., Flannery, B.P., Tuekolsky, A. and Vetterling, W.T. (1986) in Numerical Recipies: The Art of Scientific Computing, p. 287, Cambridge University Press, New York.
33 Elworthy, P.H. and MacIntosh, D.S., (1961) J. Pharm. Pharmacol. 13, 633–669.
34 Berden, J.A., Cullis, P.R., Hoult, D.I., McLaughlin, A.C., Radda, G.K. and Richards, R.E. (1974) FEBS Lett. 46, 55–58.
35 McLaughlin, A.C., Cullis, P.R., Berden, J.A. and Richards, R.E. (1975) J. Mag. Reson. 20, 146–165.
36 Meier, P., Ohmes, E. and Kothe, G. (1986) J. Chem. Phys. 85, 3598–3614.